Robust spinal cord resting-state fMRI using independent component analysis based nuisance regression noise reduction

Yong Hu, PhD[1,*], Richu Jin, ME[1], Guangsheng Li, MPhil[1,2], Keith DK Luk, MBBS[1], Ed. X. Wu, PhD [3]

[1] Department of Orthopaedics and Traumatology, Li Ka Shing Faculty of Medicine, The University of Hong Kong, Pokfulam, Hong Kong

[2] Department of Orthopaedics, Affiliated Hospital of Guangdong Medical University, Zhanjiang, China

[3] Department of Electrical and Electronic Engineering, Faculty of Engineering, The University of Hong Kong, Pokfulam, Hong Kong

[*]**Corresponding author**
Email: yhud@hku.hk Tel: +852 29740359
Address: 12 Sandy Bay Road, Department of Orthopaedics and Traumatology, Li Ka Shing Faculty of Medicine, The University of Hong Kong, Pokfulam, Hong Kong

Grant Support
This research was supported by National Science Foundation of China (81572193) and SK Yee Medical Foundation (2161216).

Competing interest
The authors have declared that no competing interests exist.

ABSTRACT

BACKGROUND： Physiological noise reduction plays a critical role in spinal cord (SC) resting-state fMRI (rsfMRI).

PURPOSE： To reduce physiological noise and increase the robustness of SC rsfMRI by using an independent component analysis (ICA) based nuisance regression (ICANR) method.

STUDY TYPE: Retrospective.

SUBJECTS: 10 healthy subjects (female/male = 4/6, age = 27±3 years, range 24 - 34 years).

FIELD STRENGTH/SEQUENCE: 3T/ Gradient-echo EPI.

ASSESSMENT: We used three alternative methods (no regression [Nil], conventional region of interest (ROI) based noise reduction method without ICA [ROI-based], and correction of structured noise using spatial independent component analysis [CORSICA]) to compare with the performance of ICANR. Reduction of the influence of physiological noise on the SC and the reproducibility of rsfMRI analysis after noise reduction were examined. Correlation coefficient (CC) was calculated to assess the influence of physiological noise. Reproducibility was calculated by intra-class correlation (ICC).

STATISTICAL TESTS: Results from different methods were compared by **o**ne-way ANOVA with post-hoc analysis.

RESULTS: No significant difference in CSF pulsation influence or tissue motion influence were found

(P=0.223 in CSF, P=0.2461 in tissue motion) in the ROI-based (CSF: 0.122±0.020; tissue motion: 0.112±0.015) and Nil (CSF: 0.134±0.026; tissue motion: 0.124±0.019). CORSICA showed a significantly stronger influence of CSF pulsation and tissue motion (CSF: 0.166±0.045, P=0.048; tissue motion: 0.160±0.032, P=0.048) than Nil. ICANR showed a significantly weaker influence of CSF pulsation and tissue motion (CSF: 0.076±0.007, P=0.0003; tissue motion: 0.081±0.014, P=0.0182) than Nil. The ICC values in the Nil, ROI-based, CORSICA, and ICANR were 0.669, 0.645, 0.561 and 0.766, respectively.

DATA CONCLUSION: ICANR more effectively reduced physiological noise from both tissue motion and CSF pulsation than three alternative methods. ICANR increases the robustness of SC rsfMRI in comparison with the other three methods.

Keywords: spinal cord, resting-state fMRI, physiological noise, independent component analysis, nuisance regression, robustness

INTRODUCTION

Spinal cord resting-state fMRI (rsfMRI) is a promising technique that offers a new way to investigate intrinsic spinal cord function in health (1-6) and disease (7,8). However, several technical challenges still hamper its clinical application. Recent studies (1-4) have adopted adjustments to rsfMRI image acquisition to successfully overcome challenges such as the small size of the spinal cord and susceptibility artifacts (9-11). One key problem that remains is non-ignorable physiological noise (12).

Spinal physiological noise can be mainly divided into non-rigid tissue motion and CSF pulsation, Tissue motion noise is mainly caused by respiration (12), and respiration-related susceptibility changes cause artifacts in rsfMRI images. These artifacts introduce intra-voxel dephasing which results in image shifting, intensity shading in the phase-encoding direction, and signal variation (13,14). These artifacts are much stronger in the spinal cord than in the brain because the spinal cord is closer to the lungs than the brain (15,16). Cardiac activity (12) leads to pulsatile movement of CSF in which the spinal cord is embedded and results in a non-rigid oscillatory cord motion (17). CSF pulsation leads to large signal variations due to unsaturated spins moving into imaging slices (18), which cannot be ignored because the spinal cord is surrounded by CSF. It has been reported that tissue motion and CSF pulsation might lead to detection of BOLD signal changes (19,20), which could generate false positive correlations in rsfMRI analysis.

Conventional physiological noise reduction method uses regions of interests (ROIs) (21). However, tissue motion is a random process so physiological noise and motion artifacts are not usually well depicted in terms of ROIs. The noise level extracted from an ROI is the average signal intensity from all voxels within the ROI (22). This averaging process makes it possible to lose the temporal features of independent noise within the ROI (23), decreasing the performance of noise extraction and reduction.

Independent component analysis (ICA) is a data-driven method to extract independent components that are mixed together in the signals. It has been recommended as a noise reduction algorithm in the brain rsfMRI because it facilitates efficient and clear separation of useful information from noise (24,25). ICA has already shown potential for noise reduction in brain rsfMRI (26-28) and spinal cord fMRI analysis (29). However, current methods cannot be directly applied to spinal cord rsfMRI for two reasons. First, existing ICA noise reduction methods select physiological noises according to its frequency (30) because differences exist between the frequencies of intrinsic BOLD signals (0.01Hz–0.1Hz) and physiological noise (0.2Hz-0.3Hz for respiration-related physiological noise and > 1Hz for cardiac-related physiological noise) in brain rsfMRI (31). Because the intrinsic BOLD signals of spinal cord rsfMRI above 0.1Hz are also important (5,6), intrinsic BOLD signals can be indistinguishable from physiological noises in that frequency domain. Second, the influence of physiological noise on variable BOLD signals would not only decrease the detectability of BOLD signals in spinal cord fMRI analysis (29) but also affect the investigation of gray matter intrinsic functional connectivity of the spinal cord by rsfMRI (32,33). As a result, the use of ICA to reduce physiological noise should be further adapted to spinal cord rsfMRI.

This issue has been addressed by Eippert et al in a review paper that suggested application of ICA to regress out physiological noise in spinal cord rsfMRI (12). Further, Oscar et al and Liu et al noticed the application of ICA without presenting its efficiency at regressing out physiological noise or its influence on the robustness of spinal cord rsfMRI investigation (3,4).

Hence, the aim of this study was to develop ICA-based nuisance regression (ICANR) as a method to reduce physiological noise and improve the robustness of cervical spinal cord rsfMRI.

MATERIAL AND METHODS

Subjects

We recruited 10 healthy subjects (6 male and 4 female, aged 24–34 years (27±3 years)). Informed consent was obtained from all participants following Institutional Review Board approval.
Subjects with normal sensory and motor functions were included. The exclusion criteria were finger flexor reflex during the physical examination, a history of traumatic injury or compressive myelopathy in the spinal cord, other neurological diseases or spinal stenosis identified in images, which were determined by professional radiologists.

Resting-state fMRI Data Acquisition

A 3-Tesla MRI machine (Philips Achieva, Amsterdam, the Netherlands) with a 16-channel neurovascular coil was used, with a gradient-echo echo planar imaging (GE-EPI) sequence. The scanning protocol was the same as that used in previously published work (4): number of slices = 26 (vertebrae C1–C7), repetition time (TR)/echo time (TE)=2000/30 ms, scan direction from head to toe, phase encoding anterior to posterior, voxel size=1.25×1.25×4 mm, scan thickness=4 mm, field of view (FOV)=80×80×104 mm, scanning time=6 min, number of volumes=180. The first five volumes were excluded because of initial transient effects.

Data Analysis

The pre-processing of rsfMRI data included slice timing, motion correction, noise reduction, detrending, and high-pass filtering (0.01 Hz), which were performed with Statistical Parametric Mapping 8 (SPM8, http://www.fil.ion.ucl.ac.uk/spm/), Resting-State fMRI Data Analysis Toolkit (REST, http://restfmri.net/forum/index.php), and Group-ICA (GIFT, http://mialab.mrn.org/software/gift/index.html) toolboxes. During motion correction, the 'realignment' function of the SPM toolbox was used to correct global motion of the FOV. For the detrending step, the REST toolbox was used to remove the BOLD signals' linear trends, avoiding false positive correlations caused by common linear trends.
During the noise reduction step, four different methods were applied for comparison. First, the ICANR method was applied to reduce physiological noise. The ICANR method included three steps: (1) by using the GIFT toolbox, spatial ICA was applied on rsfMRI data after motion correction and spatial Z-

score maps of the correlational distributions with each component were obtained (the number of components was determined by the criterion of minimum description length, which is a function embedded in the GIFT toolbox); a threshold of Z>2 was applied to the Z-score spatial maps to ignore areas having low correlations with the components; (2) physiological noise components were identified according to source location, which is defined as the area that showed the strongest correlation with noise components. The source of CSF pulsation noise components was located in the CSF area, and the source of tissue motion was located in the tissue around the cervical spinal cord, such as muscle or nerve root; (3) physiological noise components were regressed out of the rsfMRI data using the REST toolbox. Apart from physiological noise components acquired from spatial ICA, the regressor included motion correction parameters (x and y translation) (Figure 1). Second, a conventional noise reduction method (which is a nuisance regression without ICA) was applied. In this ROI-based nuisance regression, the regressor included motion correction parameters and CSF signals extracted using a CSF mask. In addition, a conventional ICA noise filtering method was performed. Third, a commonly used method called correction of structured noise using spatial independent component analysis (CORSICA) was selected for comparison. CORSICA regards independent components with high frequencies (>0.1Hz) as noises. After extracting high-frequency noises, CORSICA performs nuisance regression to regress it out. Furthermore, rsfMRI data on which nuisance regression was not performed were introduced as the control group. ICANR and ROI-based nuisance regression were the only two methods applied for noise reduction of spinal cord rsfMRI, while CORSICA was applied for noise reduction of spinal cord fMRI.

Region of Interests (ROIs) Definition

For ICANR reduction, CSF and motion source ROIs were defined. CSF ROIs were manually drawn on each slice except the first and last (Figure 2 E). Motion source ROIs were defined according to the spatial maps of tissue motion components acquired from spatial ICA. In each spatial map that includes tissue motion component, the voxel that had the strongest correlation with the tissue motion component signal was selected as the motion source ROI (Figure 2 F). Overall, 24 CSF ROIs were defined, while the number of motion source ROIs was equal to the number of tissue motion components acquired from spatial ICA.

For rsfMRI connectivity analysis, ROIs were manually drawn on the gray matter using the comparatively higher image contrast and clearer anatomy in the C2 to C6 segments (a total of 15 slices, 3 for each segment). Slices crossing the inter-vertebral discs were excluded because of FOV mismatch. Spinal cord gray matter includes the ventral horn as the motor neural pathway and the dorsal horn as the sensory neural pathway. Therefore, four ROIs were manually drawn in each slice to define the left and right sides of the ventral and dorsal horns. A total 60 ROIs were drawn for connectivity analysis (Figure 2 A-D).

Performance Evaluation of Noise Reduction

Person's correlation coefficient of the mean time series of each pair of gray matter ROIs were calculated to investigate intrinsic functional connectivity in gray matter. A 60×60 correlation matrix

was generated for each subject. Pair-wise correlation coefficients between each gray matter ROI and each CSF ROI (15 CSF ROIs per subject, on slices on which gray matter ROIs were drawn) were calculated to evaluate the interaction between gray matter and CSF and investigate the extent of influence of CSF pulsation on gray matter. A 60×15 correlation matrix was calculated for each subject to represent the influence of CSF pulsation on the gray matter. Similarly, the correlation coefficient between each gray matter ROI and each motion source ROI was calculated to investigate the extent of influence of tissue motion on the gray matter. The overall dimensions of the correlation matrix for the influence of tissue motion on the gray matter were 60×n for each subject (n is the number of tissue motion components in each subject). Higher correlation coefficients were associated with stronger influence of physiological noise on BOLD signals of the gray matter.

Statistical Analysis

For each subject, the mean value of the correlation coefficients between gray matter and CSF was calculated to represent the level of influence of CSF on the gray matter. In addition, the mean value of the correlation coefficients between gray matter and motion source ROIs was calculated to represent the level of influence of tissue motion on the gray matter. The levels of influence of both CSF and motion on the gray matter were compared by performing the following nuisance regression methods on the rsfMRI data: ICANR, CORSICA, ROI-based nuisance regression, and no nuisance regression. One-way ANOVA followed by post-hoc analysis was performed to evaluate the difference. Games-Howell method was used to correct for multiple comparison. P-values smaller than 0.05 were considered to be significant.

We tested the distribution of gray matter intrinsic functional connectivity to test whether the ICANR method affects it. Based on gray matter correlation coefficient values in each slice, four categories of gray matter intrinsic functional connectivity were established: inter-ventral, inter-dorsal, ipsilateral ventral-dorsal (left–left or right–right side), and contralateral ventral-dorsal cross side (left–right side). In a recent work, Barry et al. found robust functional connectivity between the left and right ventral horns and dorsal horns (5,6). Whether rsfMRI data after ICANR show a similar distribution (functional connectivity: correlation between left and right ventral/dorsal horns [two kinds]>correlation between ipsilateral and contralateral ventral/dorsal horns [2 kinds]) of gray matter intrinsic functional connectivity was examined by comparing the averaged correlation coefficients of these four types of gray matter intrinsic functional connectivity across all subjects.

The signals of noise-affected and noise-not-affected gray matter ROIs were compared to observe whether ICANR would process the BOLD signals not affected by noises. Considering that the affected areas were determined by the highlighted areas (Z>2, Z-transformed spatial map after spatial ICA) of the tissue motion or CSF pulsation components, the noise-affected gray matter ROIs were ones that included the affected areas (red dots in Figure 3) in terms of tissue motion or CSF pulsation components. Signal variation in gray matter ROIs that were both affected and unaffected by noise were compared after each noise reduction method was performed on the rsfMRI.

Reproducibility Test of RsfMRI Investigation

To test whether ICANR influences the intra-subject reproducibility of the rsfMRI investigation, all subjects were scanned twice with a scanning interval of 30 minutes with repositioning and re-shimming. All rsfMRI data were acquired by the same scanning protocol and underwent the same data processing as described in the methods section. Previous studies described that the strongest and most robust functional connectivity was that between left and right ventral horns (1). Therefore, to guarantee the robustness of the reproducibility test, gray matter functional connectivity between ventral horns was used to measure the reproducibility of rsfMRI. Reproducibility was calculated by intra-class correlation (ICC), which was defined as follows:

$$ICC = (BMS - EMS)/(BMS + ((k-1) * EMS))$$

where *BMS* is the between-subjects mean square, *EMS* is the error mean square and k is the number of repeated sessions.

RESULTS

Performance of Noise Reduction

Figure 3 shows the spatial maps (ICA results, Z-score transformed) of rsfMRI data after four different nuisance regression methods. In each spatial map, the voxel with the strongest correlation with the independent component (IC) may reveal the source for the IC. The tissue motion component was identified when its source of IC was located in the tissue area. Similarly, the CSF pulsation component was identified when its source of IC was located within CSF. The highlighted (red/yellow, Z>2.0) areas depicted regions with relatively strong temporal correlations with the IC, indicating influence by the IC. In the rsfMRI data on which no nuisance regression was performed, highlighted areas of gray matter in the first column of Figure 3 indicate contamination of gray matter BOLD signals by tissue motion and CSF pulsation. After ROI-based nuisance regression or CORSICA, some highlighted spots (the second column of Figure 3) were still visible in the area of the gray matter, representing the influence of tissue motion and CSF pulsation. After ICANR, little highlighted spots (the third column of Figure 3) can be seen in the area of gray matter, suggesting a clear BOLD signal estimation. Statistical analysis results showed the performance of noise reduction using different methods (Table 1). There were no significant differences between ROI-based and no nuisance regression in terms of the correlation coefficients of CSF/tissue motion with gray matter BOLD signals (P=0.223 in CSF, P=0.2461 in tissue motion). After CORSICA was performed, the correlation coefficient of CSF/tissue motion with the gray matter BOLD signals was significantly stronger than that after no nuisance regression (P=0.048). After ICANR, the correlation coefficient was significantly weaker than that after the other three methods (P=0.0182), indicating that ICANR showed the best performance of these four methods (Figure 4).

Robustness of rsfMRI after ICANR

The rsfMRI reproducibility was compared among four methods. The ICC values of no nuisance

regression, ROI-based nuisance regression, CORSICA, and ICANR were 0.669, 0.645, 0.561 and 0.766 respectively. Inter-subject variation of intrinsic functional connectivity was also compared among the fourmethods. Compared with ROI-based nuisance regression and no nuisance regression, ICANR resulted in the lowest variations of inter-ventral intrinsic functional connectivity (Figure 5).
To test whether ICANR affected the intrinsic functional connectivity, the distribution of gray matter intrinsic functional connectivity within slices was observed (Table 2). The pattern of within-slice gray matter functional connectivity distribution reported by previous studies should be inter-ventral/inter-dorsal>ipsilateral/contralateral ventral-dorsal. Inter-ventral functional connectivity was greater than the other three kinds for all three noise reduction methods. After ROI-based nuisance regression, CORSICA, and no nuisance regression, inter-dorsal functional connectivity was weaker than ipsilateral ventral-dorsal, different from the pattern shown in Figure 6A, 6B, and 6C. After ICANR was performed on the rsfMRI data, the functional connectivity strength trend was inter-ventral>inter-dorsal>ipsilateral ventral-dorsal>contralateral ventral-dorsal, which coincides with the distribution pattern shown in Figure 6D. Signal variation comparison found that ICANR did not change signals that were not affected by noises. In noise-affected gray matter ROIs, the signal after ICANR had lower signal variation than that after ROI-based nuisance regression and no regression, indicating that ICANR could reduce noise (Figure 7A). In a noise-not-affected gray matter ROI, the time series of four nuisance methods did not show the obvious difference (Fig. 7B). In both conditions, BOLD signals after CORSICA had decreased variation (Table 3).

DISCUSSION

Based on the spatial distribution of physiological noise components extracted by ICA, and ICANR method was developed for cervical spinal cord rsfMRI. Compared with no nuisance regression method, conventional ROI-based nuisance regression, and CORSICA, ICANR efficiently reduced the influence of both tissue motion and CSF pulsation on gray matter of cervical spinal cord. In addition, ICANR greatly increased the robustness of cervical spinal cord rsfMRI results, with greater intra-subject reproducibility and smaller inter-subject variations. Spinal cord rsfMRI enables new types of evaluation of spinal cord neural activity in both health and disease. This could facilitate depiction of the resting state functional neural network of the spinal cord and exploration of the motor and sensory networks inside the spinal cord. Spinal cord rsfMRI could also improve diagnosis or prognosis of cervical spinal cord neural dysfunctional diseases, such as amyotrophic lateral sclerosis (ALS), cervical spondylotic myelopathy, ossification of the posterior longitudinal ligament, and central cord syndrome. The reliable spinal cord rsfMRI investigation with assistance of ICANR may further promote the use of spinal cord rsfMRI in basic research and clinical application.

Selection of physiological noise is a crucial part of ICANR. Convincing criteria for selection of noise components can improve the accuracy of noise reduction of rsfMRI data. In this study, a threshold was applied to Z-score spatial maps to ignore areas with weak correlation with the components. In each Z-score spatial map, the voxel with the strongest correlation with the components was identified as the source. Combined with anatomic information, components with sources located in CSF were defined as CSF pulsation components; and those with sources located in tissue (e.g. muscle, nerve root) were

defined as tissue motion components. These physiological noise components selection requirements ensured that ICANR could extract reliable physiological noise components from rsfMRI data.

Another ICA-based method for spinal cord fMRI noise reduction is called CORSICA (29), which selects physiological noise components according to their frequency because of the frequency difference between physiological noises and activated BOLD signal of spinal cord fMRI (29,30). However, in spinal cord rsfMRI, the frequency band of physiological noise overlaps with the frequency band of the resting-state BOLD signal (5,6). As a result, physiological noises and resting-state BOLD signals cannot be distinguished by their frequencies. However, ICANR extracts physiological noises according to its source location. In this case, ICANR is still able to differentiate resting-state BOLD signals from physiological noise, although their frequency bands overlap.

ICANR aims to reduce tissue motion noise. The first row of Figure 3 shows red dots inside the spinal cord, which indicate a strong correlation between the spinal cord signals and the tissue motion component. In this case, there were correlations between the tissue motion noise and gray matter ROIs. If two gray matter ROIs are both correlatied with tissue motion noise, this correlation contributes to that between the two gray matter ROIs, resulting in a false positive correlation (32). This study used the signals of tissue motion ROIs (the sources of the tissue motion components) to represent tissue motion noise. The correlations between tissue motion ROIs and gray matter ROIs were used to measure the influence of tissue motion on spinal cord gray matter.

In this study, the correlation between each gray matter ROI and the motion source ROI was calculated to investigate the level of influence of tissue motion on the cervical spinal cord. ICANR is able to decrease the influence of tissue motion significantly (P=0.0182), but ROI-based nuisance regression cannot decrease it significantly (P=0.2461). CORSICA even increase the influence of tissue motion on the spinal cord. Both ROI-based nuisance regression and ICANR use motion correction parameters acquired from motion correction as regressors (34,35). These regressors mainly referred to bulk motion of the FOV, which include part of the tissue motion. Further, ICANR has more regressors than ROI-based nuisance regression. Those regressors specifically include tissue motion signals, which were different from the bulk motion of the FOV. These extra tissue motion regressors could explain why ICANR had better performance of tissue motion noise reduction than the ROI-based method. Regarding poor performance of CORSICA, because it selected high-frequency components as noises, CORSICA had a similar role of low-pass filtering. In this case, CORSICA did not address the false positive correlations caused by low-frequency components of tissue motion. This might be the reasons why CORSICA had poor performance of noise reduction. Overall, ICANR was found to efficiently reduce tissue motion noise in cervical spinal cord rsfMRI.

In this study, CSF pulsation noise was reduced by ICANR. The influence of CSF pulsation can be observed in the second row of Figure 3, as there were correlations between signals from the spinal cord and CSF (red dots inside the spinal cord). Therefore, there were correlations between CSF pulsation noise and gray matter ROIs. The correlation between two gray matter ROIs may be a false positive if both of the gray matter ROIs are correlated with CSF pulsation noise. (33,36,37). In this

study, the signals of CSF ROIs were used to represent the CSF pulsation noise. As a result, the correlations between CSF ROIs and gray matter ROIs were used to measure the influence of CSF pulsation on spinal cord gray matter.

In our study, the correlation between each gray matter and CSF ROIs were calculated to evaluate the level of influence of CSF pulsation on the cervical spinal cord. These correlations were compared among four different methods. The rsfMRI data after ICANR showed less CSF pulsation influence than either ROI-based nuisance regression or no regression. CORSICA even increased the influence of CSF pulsation on the spinal cord. These results indicated that ICANR effectively reduces the influence of CSF pulsation on the cervical spinal cord. Both ROI-based nuisance regression and the ICANR method included regression of CSF signals. In ROI-based nuisance regression, the CSF signals were extracted from a CSF mask, while the CSF signals from ICANR were independent noise components extracted by spatial ICA. CSF pulsations in the spinal cord canal are independent because they are not uniform and have different velocities (38). This characteristic corresponds to the independent CSF components extracted from spatial ICA. As a result, regressing out the independent CSF pulsation signals may regress out all possible components of CSF pulsations. In ROI-based method, CSF signal extracted from a CSF ROI was the average of signals from all voxels within the CSF ROI. The averaging process made it possibility to average the independent CSF pulsation signals inside each CSF ROI. Thus, the averaged CSF signal may lose the temporal feature of independent CSF pulsation signals (23). As a result, it may reduce the performance of CSF pulsation noise reduction. The reason for poor performance of CORSICA may be its inability to handle false positive correlations caused by low-frequency components of CSF pulsation. Our results indicated that ICANR can efficiently reduce CSF pulsation noise in cervical spinal cord rsfMRI.

In this study, measurement of the robustness of rsfMRI investigation after ICANR included two aspects: intra-subject reproducibility and inter-subject variability. Results of intra-subject reproducibility showed that ICANR had the highest intra-class correlation coefficient in the rsfMRI investigation. Meanwhile, the inter-subject variability comparison indicated that ICANR had the lowest intrinsic functional connectivity variation among four methods. Both the increased intra-subject reproducibility and decreased inter-subject variability indicate that ICANR provides high robustness in cervical spinal cord rsfMRI investigation, which further verifies its reduction of the influence of physiological noise.

To investigate whether ICANR distorts results of the rsfMRI analysis, the intrinsic functional connectivity distribution among gray matter ROIs within each slice was summarized. Figure 6 shows that inter-ventral functional connectivity was stronger than the other three methods. However, after no nuisance regression, ROI-based nuisance regression, and CORSICA, inter-dorsal was weaker than ipsilateral ventral-dorsal functional connectivity, which was not consistent with the pattern reported by other studies (5,6). After ICANR was performed on the rsfMRI data, inter-dorsal was stronger than ipsilateral ventral-dorsal functional connectivity, which was consistent with the findings of previous studies (5,6). The intrinsic functional connectivity distribution pattern without nuisance regression was the pattern in which physiological noises was not reduced. ROI-based nuisance regression and CORSICA generated similar patterns to that of no nuisance regression, which might indicate that the

rsfMRI data were still affected by residual physiological noises. The pattern of intrinsic functional connectivity after ICANR was consistent with the findings of previous studies, indicating that the influence of physiological noise had been reduced.

Our observation indicated that not all gray matter ROIs were affected by physiological noise because some gray matter ROIs did not show strong correlations with CSF pulsation or tissue motion. To test whether ICANR will over-process BOLD signal when they are not affected by noises, signals from noise-affected and noise-not-affected gray matter ROIs were compared. In the noise-affected gray matter ROIs, the signals after ICANR showed lower variations than those of three alternative methods. In the gray matter ROI that were not affected by noise, the signals did not show obvious difference among four methods. This implies that ICANR only reduces physiological noises in the affected gray matter area and will not over-process BOLD signal. However, in both conditions, BOLD signals after CORSICA all present decreased variations, indicating that CORSICA may over-process BOLD signals.

This study focused on noise reduction, rather than each step of rsfMRI processing (6,12,19). Future studies will focus on the performance of all possible methods in each step of rsfMRI processing. Furthermore, the selection of physiological noise was made manually in this study. Automatic noise selection methods, which should be developed for ICANR in future studies, can reduce the time required for processing (26,39,40). With the development of spinal cord rsfMRI technology, there will be future study on new noise reduction methods other than the proposed ICANR.

In conclusion, we have developed an ICANR method to reduce physiological noise in spinal cord rsfMRI. Compared with conventional ROI-based nuisance regression, CORSICA, and no regression methods, the ICANR efficiently reduced the influence of both tissue motion and CSF pulsation on gray matter. As a result, ICANR greatly increased the robustness of cervical spinal cord rsfMRI investigation, showing greater intra-subject reproducibility and smaller inter-subject variations. Our results indicate that ICANR is an effective method to reduce physiological noise and improve the robustness of spinal cord rsfMRI. The ICANR method enables more accurate investigation of spinal cord intrinsic functional connectivity, which may deepen our understanding of the entire human nervous system. This study demonstrates the use of ICANR method for the robust spinal cord rsfMRI.

ACKNOWLEDGEMENTS

Contract grant sponsor: National Science Foundation of China; contract grant number: 81572193; Contract grant sponsor: SK Yee Medical Foundation; contract grant number: 2161216 We thank Mr Xiaojia Liu for his assistance in image processing and graph preparation; Liwen Bianji, Edanz Group China (www.liwenbianji.cn/ac), for editing the English text of the article.

REFERENCES

1. Barry RL, Smith SA, Dula AN, Gore JC. Resting state functional connectivity in the human spinal cord. Elife 2014;3:e02812.
2. Kong Y, Eippert F, Beckmann CF, et al. Intrinsically organized resting state networks in the human spinal cord. Proc Natl Acad Sci U S A 2014;111(50):18067-18072.
3. San Emeterio Nateras O, Yu F, Muir ER, et al. Intrinsic Resting-State Functional Connectivity in the Human Spinal Cord at 3.0 T. Radiology 2016;279(1):262-268.
4. Liu X, Zhou F, Li X, et al. Organization of the intrinsic functional network in the cervical spinal cord: A resting state functional MRI study. Neuroscience 2016;336:30-38.
5. Barry RL, Rogers BP, Conrad BN, Smith SA, Gore JC. Reproducibility of resting state spinal cord networks in healthy volunteers at 7 Tesla. Neuroimage 2016;133:31-40.
6. Eippert F, Kong Y, Winkler AM, et al. Investigating resting-state functional connectivity in the cervical spinal cord at 3T. Neuroimage 2016;147:589-601.
7. Chen LM, Mishra A, Yang PF, Wang F, Gore JC. Injury alters intrinsic functional connectivity within the primate spinal cord. Proc Natl Acad Sci U S A 2015;112(19):5991-5996.
8. Liu X, Qian W, Jin R, et al. Amplitude of Low Frequency Fluctuation (ALFF) in the Cervical Spinal Cord with Stenosis: A Resting State fMRI Study. PLoS One 2016;11(12):e0167279.
9. Giove F, Garreffa G, Giulietti G, Mangia S, Colonnese C, Maraviglia B. Issues about the fMRI of the human spinal cord. Magn Reson Imaging 2004;22(10):1505-1516.
10. Stroman PW, Wheeler-Kingshott C, Bacon M, et al. The current state-of-the-art of spinal cord imaging: methods. Neuroimage 2014;84:1070-1081.
11. Summers PE, Iannetti GD, Porro CA. Functional exploration of the human spinal cord during voluntary movement and somatosensory stimulation. Magn Reson Imaging 2010;28(8):1216-1224.
12. Eippert F, Kong Y, Jenkinson M, Tracey I, Brooks JC. Denoising spinal cord fMRI data: Approaches to acquisition and analysis. Neuroimage 2016.
13. Raj D, Anderson AW, Gore JC. Respiratory effects in human functional magnetic resonance imaging due to bulk susceptibility changes. Phys Med Biol 2001;46(12):3331.
14. de Moortele V, Pfeuffer J, Glover GH, Ugurbil K, Hu X. Respiration-induced B0 fluctuations and their spatial distribution in the human brain at 7 Tesla. Magn Reson Med 2002;47(5):888-895.
15. Verma T, Cohen-Adad J. Effect of respiration on the B0 field in the human spinal cord at 3T. Magn Reson Med 2014;72(6):1629-1636.
16. Brooks JC, Beckmann CF, Miller KL, et al. Physiological noise modelling for spinal functional magnetic resonance imaging studies. Neuroimage 2008;39(2):680-692.

17. Figley CR, Stroman PW. Investigation of human cervical and upper thoracic spinal cord motion: implications for imaging spinal cord structure and function. Magn Reson Med 2007;58(1):185-189.
18. Finsterbusch J, Eippert F, Buchel C. Single, slice-specific z-shim gradient pulses improve T2*-weighted imaging of the spinal cord. Neuroimage 2012;59(3):2307-2315.
19. Kong Y, Jenkinson M, Andersson J, Tracey I, Brooks JC. Assessment of physiological noise modelling methods for functional imaging of the spinal cord. Neuroimage 2012;60(2):1538-1549.
20. Welvaert M, Rosseel Y. How ignoring physiological noise can bias the conclusions from fMRI simulation results. J Neurosci Methods 2012;211(1):125-132.
21. Lee MH, Smyser CD, Shimony JS. Resting-state fMRI: a review of methods and clinical applications. AJNR Am J Neuroradiol 2013;34(10):1866-1872.
22. Constantinides CD, Atalar E, McVeigh ER. Signal-to-noise measurements in magnitude images from NMR phased arrays. Magn Reson Med 1997;38(5):852-857.
23. Ben-Yakov A, Honey CJ, Lerner Y, Hasson U. Loss of reliable temporal structure in event-related averaging of naturalistic stimuli. Neuroimage 2012;63(1):501-506.
24. Beckmann CF. Modelling with independent components. Neuroimage 2012;62(2):891-901.
25. Starck T, Remes J, Nikkinen J, Tervonen O, Kiviniemi V. Correction of low-frequency physiological noise from the resting state BOLD fMRI—Effect on ICA default mode analysis at 1.5 T. J Neurosci Methods 2010;186(2):179-185.
26. Salimi-Khorshidi G, Douaud G, Beckmann CF, Glasser MF, Griffanti L, Smith SM. Automatic denoising of functional MRI data: combining independent component analysis and hierarchical fusion of classifiers. Neuroimage 2014;90:449-468.
27. Boubela RN, Kalcher K, Huf W, Kronnerwetter C, Filzmoser P, Moser E. Beyond Noise: Using Temporal ICA to Extract Meaningful Information from High-Frequency fMRI Signal Fluctuations during Rest. Front Hum Neurosci 2013;7:168.
28. Moher Alsady T, Blessing EM, Beissner F. MICA—A toolbox for masked independent component analysis of fMRI data. Hum Brain Mapp 2016;37(10):3544-3556.
29. Xie G, Piche M, Khoshnejad M, et al. Reduction of physiological noise with independent component analysis improves the detection of nociceptive responses with fMRI of the human spinal cord. Neuroimage 2012;63(1):245-252.
30. Perlbarg V, Bellec P, Anton JL, Pelegrini-Issac M, Doyon J, Benali H. CORSICA: correction of structured noise in fMRI by automatic identification of ICA components. Magn Reson Imaging 2007;25(1):35-46.
31. Tong Y, Lindsey KP, de BFB. Partitioning of physiological noise signals in the brain with concurrent near-infrared spectroscopy and fMRI. J Cereb Blood Flow Metab 2011;31(12):2352-2362.
32. Birn RM, Diamond JB, Smith MA, Bandettini PA. Separating respiratory-variation-related fluctuations from neuronal-activity-related fluctuations in fMRI. Neuroimage 2006;31(4):1536-1548.
33. Chang C, Cunningham JP, Glover GH. Influence of heart rate on the BOLD signal: the cardiac response function. Neuroimage 2009;44(3):857-869.

34. Hahn AD, Rowe DB. Physiologic noise regression, motion regression, and TOAST dynamic field correction in complex-valued fMRI time series. Neuroimage 2012;59(3):2231-2240.
35. Power JD, Schlaggar BL, Petersen SE. Recent progress and outstanding issues in motion correction in resting state fMRI. Neuroimage 2015;105:536-551.
36. Lund TE. fcMRI—Mapping functional connectivity or correlating cardiac-induced noise? Magn Reson Med 2001;46(3):628-628.
37. Shmueli K, van Gelderen P, de Zwart JA, et al. Low-frequency fluctuations in the cardiac rate as a source of variance in the resting-state fMRI BOLD signal. Neuroimage 2007;38(2):306-320.
38. Piché M, Cohen-Adad J, Nejad MK, et al. Characterization of cardiac-related noise in fMRI of the cervical spinal cord. Magn Reson Imaging 2009;27(3):300-310.
39. Sochat V, Supekar K, Bustillo J, Calhoun V, Turner JA, Rubin DL. A robust classifier to distinguish noise from fMRI independent components. PLoS One 2014;9(4):e95493.
40. Pruim RH, Mennes M, van Rooij D, Llera A, Buitelaar JK, Beckmann CF. ICA-AROMA: a robust ICA-based strategy for removing motion artifacts from fMRI data. Neuroimage 2015;112:267-277.

Tables

Table 1 Influence of CSF/tissue motion on the gray matter after different noise reduction methods

	No Regression	ROI-based	CORSICA	ICANR
CSF pulsation influence	0.134±0.026	0.122±0.020	0.166±0.045	0.076±0.007
Tissue motion influence	0.124±0.019	0.112±0.015	0.160±0.032	0.081±0.014

Note: no regression – no nuisance regression; ROI-based – ROI-based nuisance regression; CORSICA - correction of structured noise using spatial independent component analysis; ICANR – ICA-based nuisance regression.

Table 2 summary of the distribution of gray matter intrinsic functional connectivity within slices (mean±std)

	No Regression	ROI-based	CORSICA	ICANR
Inter-ventral	0.230±0.233	0.243±0.210	0.194±0.233	0.189±0.131
Inter-dorsal	0.095±0.179	0.096±0.152	0.085±0.195	0.107±0.134
Ipsilateral ventral-dorsal	0.111±0.197	0.106±0.169	0.126±0.207	0.057±0.144
Contralateral ventral-dorsal	0.058±0.179	0.052±0.154	0.069±0.194	0.017±0.121

Note: no regression – no nuisance regression; ROI-based – ROI-based nuisance regression; CORSICA - correction of structured noise using spatial independent component analysis; ICANR – ICA-based nuisance regression.

Table 3 Signal variations in noise-affected and noise-not-affected gray matter ROIs (std)

	No Regression	ROI-based	CORSICA	ICANR
Noise-affected gray matter	249.3	218.3	106.7	151.5
Noise-not-affected gray matter	87.6	86.9	38.7	85.6

Note: no regression – no nuisance regression; ROI-based – ROI-based nuisance regression; CORSICA - correction of structured noise using spatial independent component analysis; ICANR – ICA-based nuisance regression.

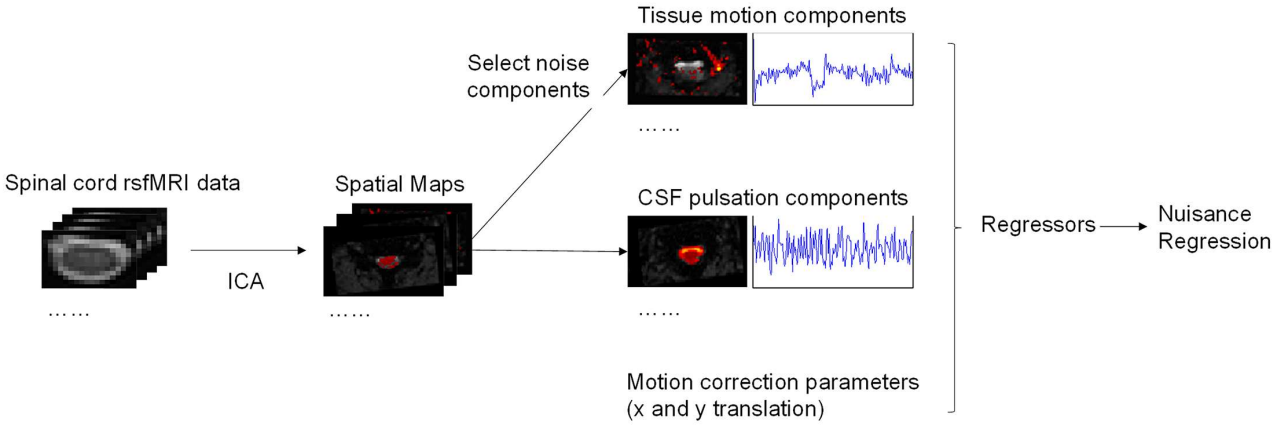

Figure 1. Method of ICA-based nuisance regression (ICANR). rsfMRI data firstly performed spatial ICA to get spatial maps. Noise components were selected out and their signals were combined with motion correction parameters to establish regressors. Nuisance regression was finally performed to regress out noise based on the established regressors.

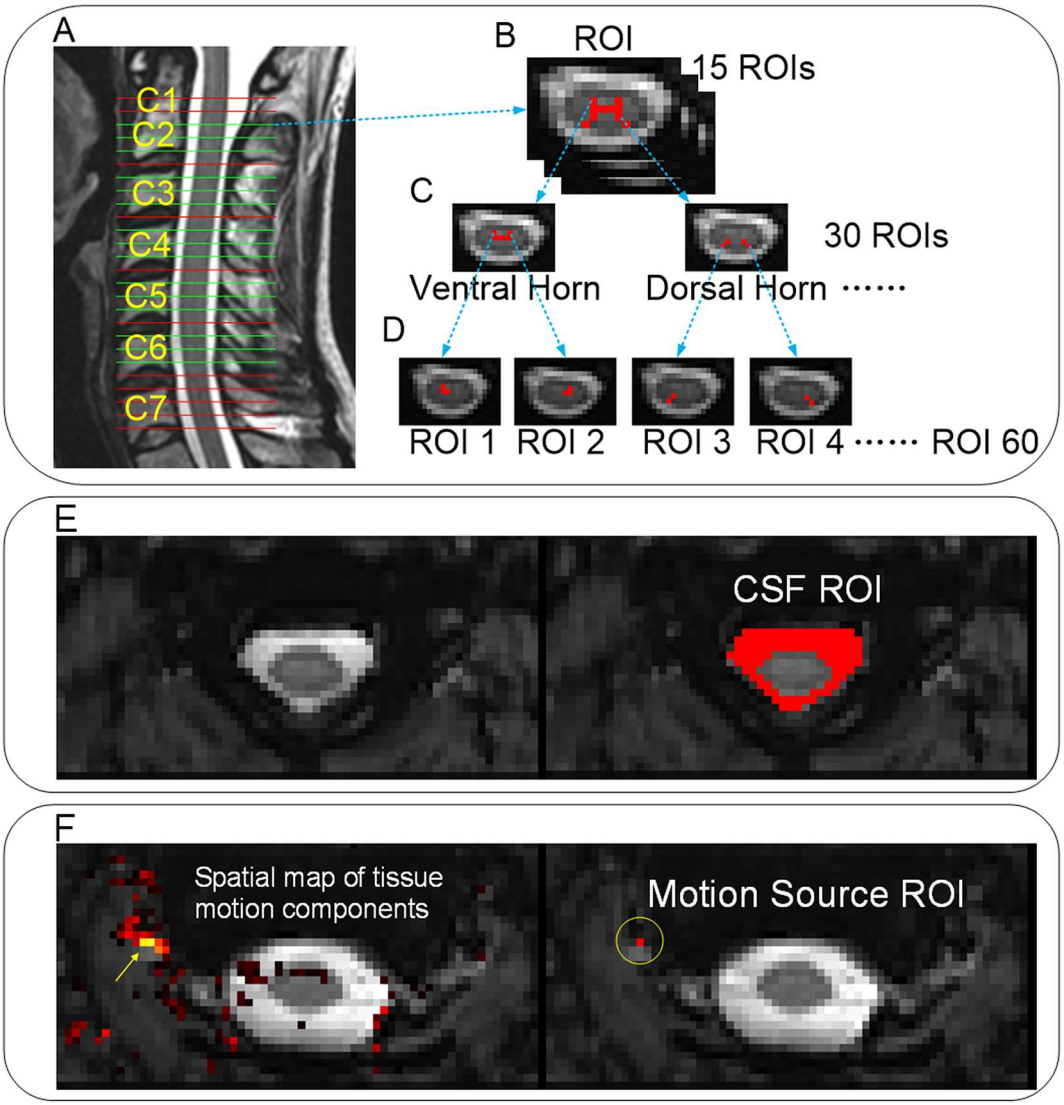

Figure 2. Gray matter regions of interest (ROIs) definition in the cervical spinal cord. The rsfMRI scanning field of view (FOV) and slice location that cover vertebrae C1 to C7 (A); the gray matter was drawn on post-processed echo planar imaging (EPI) images (B); the gray matter ROI was then delineated and split into ROI1 (ventral horn) and ROI2 (dorsal horn) (C); left and right parts of each horn were also furtherly separated; finally 60 ROIs were extracted from each subject (D). CSF ROIs were also manually drawn on each slice except for first and last slice (E). Based on the spatial maps of tissue motion components acquired from spatial ICA, the voxel that had the highest correlation (yellow arrow) with tissue motion component signal was selected as motion source ROI (F).

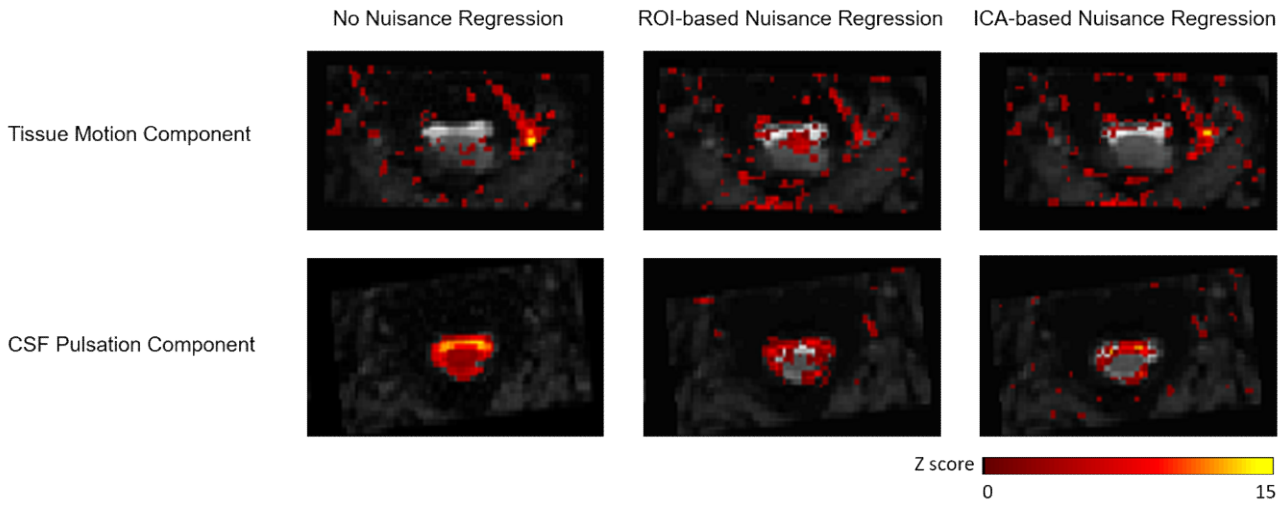

Figure 3. Spatial maps (ICA results, Z-score transformed) of rsfMRI data after four different nuisance regression methods. In each spatial map, the voxel with highest correlation to independent component (IC) may reveal the source of IC. For tissue motion component, the voxel have highest correlation to IC is located at the tissue area. The CSF pulsation component have the voxel with highest correlation to IC that located at CSF area. The highlighted (red/yellow, $|z|>2.0$) areas depicted regions that have relatively high temporal correlation to IC. The yellow areas may represent the source of the independent component signal. In each figure, the yellow circle is the spinal cord area. The red dots in yellow circle indicated that the spinal cord have high correlation with the independent component signal, which means the spinal cord was affected by the independent component. RsfMRI data that did not perform nuisance regression will be affected by tissue motion and CSF pulsation. ROI-based nuisance regression could decrease the influence but the gray matter was still affected. CORSICA did not decrease the influence. ICA-based nuisance regression could decrease the influence of both tissue motion and CSF pulsation clearly. Note: no regression – no nuisance regression; ROI-based – ROI-based nuisance regression; CORSICA - correction of structured noise using spatial independent component analysis; ICANR – ICA-based nuisance regression.

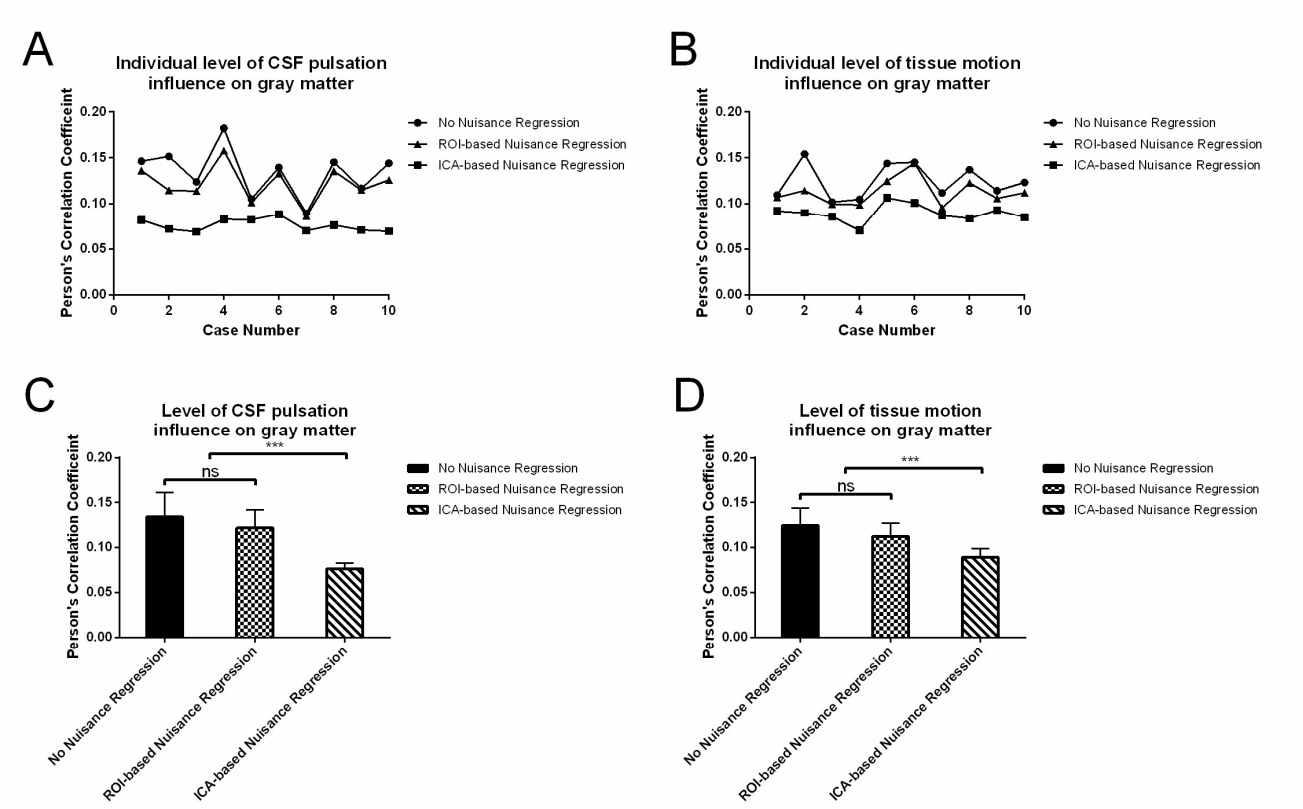

Figure 4. Statistical analysis about the level of CSF pulsation and tissue motion influence on gray matter. For individual comparison, compared with no nuisance regression, ROI-based nuisance regression did not have an obvious difference on CSF pulsation influence and tissue motion influence. The ICA-based nuisance regression has an obvious weaker influence of both CSF pulsation and tissue motion influence (A, B). For group comparison, ROI-based nuisance regression did not have a significantly different influence of CSF and tissue motion. CORSICA have a significantly stronger influence of CSF and tissue motion. ICA-based nuisance regression has the significant weaker influence of both CSF pulsation and tissue motion in comparison with no nuisance regression and ROI-based nuisance regression. Note: no regression – no nuisance regression; ROI-based – ROI-based nuisance regression; CORSICA - correction of structured noise using spatial independent component analysis; ICANR – ICA-based nuisance regression.

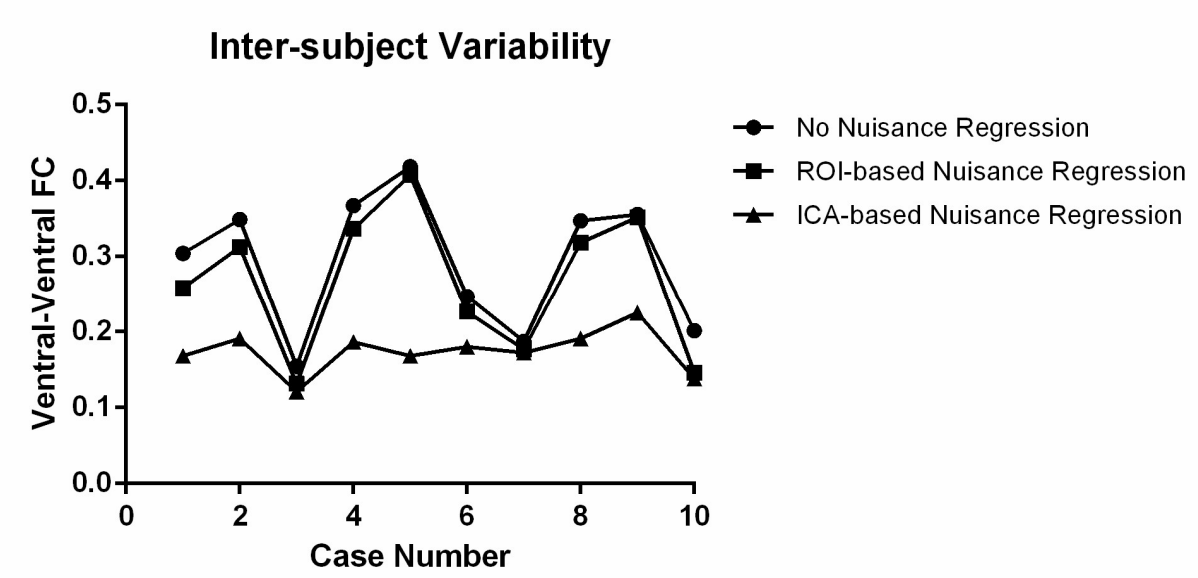

Figure 5. Inter-subject variability comparison of inter-ventral intrinsic functional connectivity after rsfMRI data performed four different nuisance regression methods. ICA-based nuisance regression method showed lowest variations of inter-ventral functional connectivity among all subjects, which means that ICA-based nuisance regression method has the lowest inter-subject variability. Note: no regression – no nuisance regression; ROI-based – ROI-based nuisance regression; CORSICA - correction of structured noise using spatial independent component analysis; ICANR – ICA-based nuisance regression.

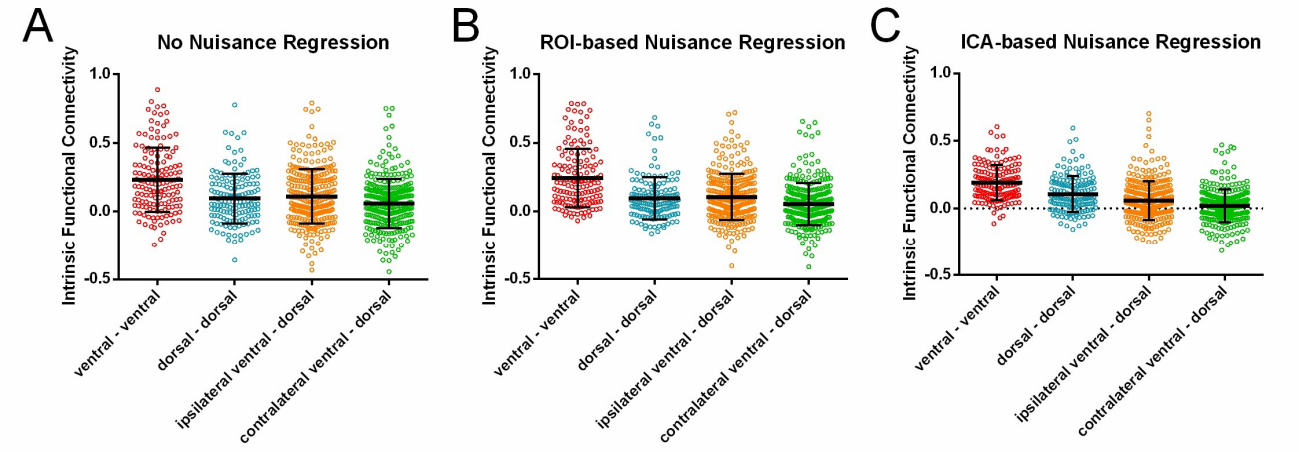

Figure 6. Distribution of gray matter intrinsic functional connectivity after rsfMRI data performed four different nuisance regression methods. Inter-ventral and inter-dorsal have stronger intrinsic functional connectivity values than ipsilateral ventral-dorsal and contralateral ventral-dorsal after rsfMRI data performed ICA-based nuisance regression. The rest three methods only showed obvious stronger inter-ventral intrinsic functional connectivity than the rest three kinds of intrinsic functional connectivity. Note: no regression – no nuisance regression; ROI-based – ROI-based nuisance regression; CORSICA - correction of structured noise using spatial independent component analysis; ICANR – ICA-based nuisance regression.

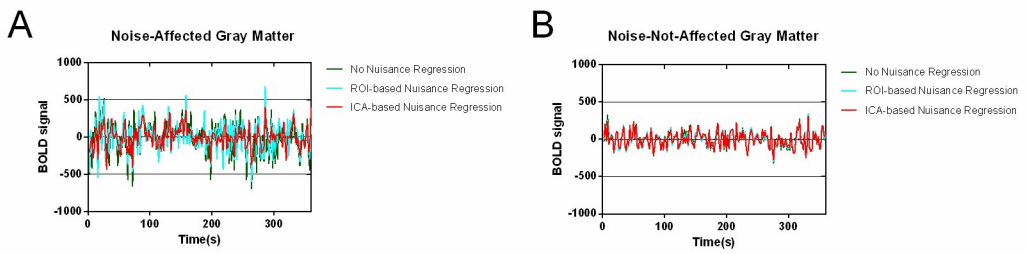

Figure 7. An example of the signal from both noise- affected and noise-not-affected gray matter ROIs. In the noise-affected gray matter ROI, time series after ICA-based nuisance regression exhibited lower signal variations than no nuisance regression and ROI-based nuisance regression (A). In the noise-not-affected gray matter ROI, time series did not have an obvious difference among these three methods (B). In both conditions, BOLD signals after CORSICA all present decreased variations. Note: no regression – no nuisance regression; ROI-based – ROI-based nuisance regression; CORSICA - correction of structured noise using spatial independent component analysis; ICANR – ICA-based nuisance regression.